Gold Nanoparticles Conjugated with Cisplatin/Doxorubicin/ Capecitabine Lower the Chemoresistance of Hepatocellular Carcinoma-Derived Cancer Cells

Ciprian Tomuleasa[1,2,3], Olga Soritau[2], Anamaria Orza[4], Mircea Dudea[4], Bobe Petrushev[5], Ofelia Mosteanu[6], Sergiu Susman[7], Adrian Florea[8], Emoke Pall[9], Mihaela Aldea[5], Gabriel Kacso[10,11], Victor Cristea[3,6], Ioana Berindan-Neagoe[3,12], Alexandru Irimie[13,14]

1) Department of Medicine, Division of Gastroenterology and Hepatology, The Johns Hopkins University School of Medicine, Baltimore, MD, USA; Departments of 2) Cancer Immunology; 11) Radiotherapy; 13) Genetics; 14) Surgery, Ion Chiricuta Comprehensive Cancer Center; 4) Faculty of Chemistry, Babes-Bolyai University; Departments of 4) Immunology; 5) Medicine; 6) Gastroenterology, 8) Histology; 9) Cell and molecular biology; 12) Oncology; 15) Surgical Oncology, Iuliu Hatieganu University of Medicine and Pharmacy; 7) Department of Gastroenterology, Prof. Octavian Fodor Regional Institute of Gastroenterology and Hepatology; 10) Faculty of Veterinary Medicine, University of Veterinary Medicine and Agricultural Sciences, Cluj Napoca, Romania

Abstract

Background & Aims: The aim of the current study was to evaluate in vitro the anti-tumor efficacy of gold nanoparticles (GNPs) conjugated with conventional chemotherapy drugs for the treatment of liver cancer. This approach based on gold proposes a novel platform therapy with minimal toxicity and increased efficacy profiles for the destruction of hepatic cancer cells. **Methods**. GNPs, stabilized with a monolayer of L-aspartate and additional cytostatic drugs, were successfully used as a complex tumor-targeting drug-delivery system. The drugs (doxorubicin, cisplatin, and capecitabine) were non-covalently conjugated onto the hydrophilic assemblies of GNPs-L-Aspartate nanostructure. Transmission electron microscopy was used to characterize the morphological and structural properties of these drug-metallic nanostructures. **Results.** The cellular proliferation rates in the presence of the anti-cancer drugs delivered by the GNPs were found to be statistically lower than those of cells exposed to the cytostatic drugs alone, indicating that GNPs facilitated an increased susceptibility of cancer cells to cisplatin, doxorubicin, and capecitabine plus ribavirin. **Conclusion**. This approach could offer a new chemotherapy strategy for patients diagnosed with unresectable hepatocellular carcinoma (HCC).

Received: 02.12.2011 Accepted: 03.04.2012
J Gastrointestin Liver Dis
June 2012 Vol. 21 No 2, 187-196
Address for correspondence: CiprianTomuleasa
Dept. of Medicine
Div. Gastroenterol Hepatol
The Johns Hopkins University
School of Medicine,
Baltimore, MD, USA
ciprian.tomuleasa@gmail.com
ctomule1@jhmi.edu

Key words

Gold nanostructures – drug-delivery systems – cancer cells – hepatocellular carcinoma.

Abbreviations

GNPs: gold nanoparticles; TEM: transmission electron microscopy; NMR: nuclear magnetic resonance; HCC: hepatocellular carcinoma; CSC: chemotherapy-resistant cancer cells; LIV: normal non-cancerous liver cells; PBS: phosphate buffered saline; CD133: glycoprotein also known as Prominin 1; CD 90: Cluster of Differentiation 90; ABCG2: ATP-binding Cassette G2 protein; GAPDH: glyceraldehyde 3-phosphate dehydrogenase; EDTA: Ethylenediaminetetraacetic acid; MTT: 3-(4,5-Dimethylthiazol-2-yl)-2,5-diphenyltetrazolium bromide; PI: propidium iodide; PIAF protocol: Planning-, Information- and Analysis-System for Field Trials protocol; P-gp: P-glycoprotein.

Introduction

According to GLOBOCAN 2000, "Hepatocellular carcinoma (HCC) is the fifth most common solid tumor worldwide and the fourth leading cause of cancer-related death," with an estimated death rate of more than 500,000 per year [1]. The disease is usually detected when the tumor is in an advanced stage and surgical resection is in most cases no longer feasible. Liver transplantation is normally the best option, as long as the patient still falls within the Milan criteria [2]. Without surgical intervention, survival depends on the amount of healthy liver tissue remaining in comparison with cirrhotic or malignant tissue (Child-Pugh grade and tumor stage). Existing liver cancer treatments,

including loco-regional or systemic chemotherapy, fail largely due to the chemoresistance properties of cancer cells, as well as their ability to stimulate neoangiogenesis [3]. The most successful form of treatment comprises the combination chemotherapy of doxorubicin, cisplatin, and 5-fluorouracil plus interferon α-2b [4]. The original protocol of Yeo at al was later slightly modified by replacing fluorouracil with capecitabine [5], or even antiviral therapy using ribavirin, in the cases of hepatocellular carcinomas that appear after a chronic hepatitis C infection and cirrhosis [6,7]. However, high doses of drugs lead to systemic toxicity resulting in nausea, vomiting, renal failure, peripheral neuropathy, asthenia, and/or cytotoxicity [8]. The multitude of unwanted adverse reactions to classical anticancer drugs, their lack of availability at the tumor site, poor tumor intake of drugs and rapid elimination are some of the primary difficulties involved in treating any form of cancer [9].

Since tumors are believed to develop resistance to chemotherapy shortly after the first chemotherapy regimens [10], new approaches are required that can specifically kill at the level of the individual cancer cell in order to control and reduce the progression and spreading of these cells in the body. Engineered nanostructured materials have recently been proposed as components of multifunctional cancer treatment platforms given their ability to deliver drugs and genes, as well as to induce heat-hyperthermia. In particular, gold nanoparticles (GNPs) could provide a significant opportunity for novel medical treatments due to their facile preparation, low toxicity, and anti-angiogenic properties, as well as their ability to bind with various target bio-chemical molecules [11].

Developments in nanotechnology could offer novel approaches capable of detecting cancer and delivering antineoplastic drugs to individual cancer cells [12]. During the course of the past ten years, a variety of nanomaterials - polymers, dendrimers, liposomes, nanotubes, and nanorods have been used as the basis for drug-delivery vehicles [13]. The payloads can vary from small drug molecules to large biomolecules like proteins, DNA, or RNA [14-23].

In this study, we present the synthesis and characterization of GNPs-L-Aspartate nanostructures functionalized with chemotherapeutic drugs used for successful HCC therapy. Differentiated cancer cells derived from human HCC (HepG2 cell line), chemotherapy-resistant cancer cells isolated from hepatocellular carcinoma (CSC), and normal non-cancer liver cells (LIV) were exposed in vitro to GNP-conjugated anticancer drugs. By providing new anticancer therapies to hepatocellular carcinoma, this approach could represent a novel form of cancer treatment and, in particular, decrease the chemoresistance developed by cancer cells to commonly used cytostatic drugs.

Materials and Methods

GNPs-L- Aspartate nanostructures

Tetrachloroauric acid (HAuCl4) cisplatin, capecitabine, and doxorubicin were purchased from Fluka (Sigma-Aldrich Inc.) and L-Aspartate from Merck. HAuCl4 and L-Aspartic acid solutions were prepared in concentrations (C) of $0.5x10^{-3}$M and $1.5x10^{-3}$M, respectively. The synthesis of gold nanostructures commenced by mixing stoichiometric volumes of [$HAuCl_4$]/[Acid aspartic] of 1/1, as follows: over 50 ml boiled solution of HAuCl4, C=$0.5x10^{-3}$M, a solution of 15 ml C=$1.5x10^{-3}$ M aspartic acid was added. A change of color from yellow to red occurred, after which the solution was allowed to rest at room temperature for 24h. The resulting product was twice centrifuged at 15,000 rpm for 45 minutes, washed with double distilled water, and finally redispersed in phosphate buffered saline (PBS) to a final concentration of 3 nM. Further, the aspartic nanostructures were functionalized with the desired drugs (cisplatine, capecitabine, doxorubicin). In an ice bath and vigorous mixing conditions, over 10 ml gold nanostructures solution were added 500 µl of drug, C=(50 µg/ml). The solution was mixed for 1 hour. The resulting compound was centrifuged three times at 15,000 rpm for 1 hour and washed with PBS. After centrifugation, the compound was redispersed in PBS to a final concentration of 5 µg/ml. The morphology of the GNPs-nanostructures and that of drug delivery was investigated by transmission electron microscopy (TEM). Droplets of 30µL suspension were pipetted on copper grids (3 mm diameter, 300 meshes) previously covered with parlodion and carbon films. After 2 minutes, the extra liquid was absorbed with filter paper. Examination of the sample containing grids was performed on a Jeol JEM 1010 transmission electron microscope (Jeol, Tokyo, Japan). The images were captured using a Mega VIEW III camera (Olympus, Soft Imaging System, Münster, Germany) and introduced in a database using the Soft Imaging System software (Soft Imaging System, Münster, Germany). The diameter of nanoparticles was analyzed using the CellD software (Olympus Soft Imaging Solutions GMBH, Münster, Germany).

Cell culture

Cancer cells (CSC) isolated from a hepatocellular carcinoma biopsy, as previously described, expressed specific markers including CD133, CD90, Oct ¾, Nanog, ABCG2, or GAPDH. The primary cultures represented by CSC and normal liver cells (LIV) were maintained in Ham's F-12 and Dulbecco's Modified Essential Medium at 1:1 ratio, supplemented with 15% fetal calf serum (FCS), 100 U/mL penicillin, and 100 µg/mL streptomycin, 1% non-essential aminoacids, 2mM glutamine, 55µM beta-mercaptoethanol, 1mM natrium piruvate in a 37°C humidified incubator with a mixture of 95% air and 5% carbon dioxide. The classic tumor cell line HepG2 was cultivated in RPMI medium with 10% fetal calf serum (FCS), 100U/mL penicillin, 100µg/mL streptomycin, and 2mM L-glutamine. All reagents were purchased from Sigma Aldrich, St Louis, MO, USA. All experiments were performed on exponentially growing cells, with a doubling time of approximately 24 to 36 hours. For the passage, the medium was discarded, and cells were washed with phosphate buffer solution and afterwards detached with trypsin/ 0.25% EDTA.

Microscopy images (both white light microscopy and fluorescence microscopy at 488 nm) were taken using a Zeiss Axiovert inverted phase microscope, equipped with soft image analysis Axiovision Rel 4.6. Image acquisition was performed with an AxioCam MRC camera.

Transmission Electron Microscopy (TEM) of the cells

After 1 h of incubation with the functionalized drugs, the cells were fixed by the addition of 4% paraformaldehyde/2.5% glutaraldehyde in phosphate buffer (0.7 ml) for 1 h. The cells were next rinsed with PBS buffer and post-fixed using 1% aqueous solution of OsO4 (0.5 ml) for 1 h. Subsequently, the cells were washed with milli-Q H20, 30% ethanol solution and stained with 0.5% uranyl acetate (0.5 ml, in 30% ethanol) for 1 h. Cells were then gradually dehydrated using a series of ethanol solutions (30, 60, 70, 80, and 100%) and embedded in epoxy resin. The resin was polymerized at 60˚C for 48 h. Ultra-thin sections (70-100 nm) were cut using a diamond knife on a Leica Ultramicrotome and mounted on Formvar-coated copper grids. The sections were then post-stained with 5% uranyl acetate in 50% ethanol and 2% aqueous lead citrate solution and imaged with FEI Tecnai Spirit TEM at 100 kV using AnalySIS software (Soft Imaging Systems).

Proliferation assay

Cell survival was assessed using the MTT assay. For 3-(4,5-Dimethylthiazol-2-yl)-2,5-diphenyltetrazolium bromide (MTT) assays, CSC, LIV, and HepG2 cells in monolayer culture were cultivated at subconfluence in DMEM:F-12 media supplemented with 15% FCS, 100 U/mL penicillin, and 100µg/mL streptomycin complete media before being washed twice with phosphate buffer solution (PBS). Cells were then incubated with trypsin-EDTA, resuspended in culture medium with FCS, counted, and plated in 100 µL media at 15 x 10^3 cells/well in 96-well microliter plates. After 24 hours, the cells were washed and treated with cytostatic drugs. Doxorubicin was added at a concentration of 0.5 µg/ml, cisplatin at 0.25 µg/ml, and capecitabine at 30 µg/ml [4,5]. The concentrations that were used are in conjugation with GNPs, after extensive pilot projects (data not shown in this paper) have been completed and having established the best concentrations of drugs that should be used. Drug-capped GNPs were compared with the corresponding conventional cytostatics at identical concentrations. Absorbance of the MTT was measured at 492 nm using a BioTek Synergy 2 fluorescence microplate reader (Winooski, VT, USA).

Apoptosis measurement using Annexin/PI flow cytometry analysis

To further investigate the role of the GNPs in enhancing the drug activity in various cell lines, CSC and LIV were grown at subconfluence in 6-well plates and were exposed for 24 hours to a combination of chemotherapeutic drugs conjugated or unconjugated with GNPs (doxorubicin 0.5 µg/ml+ cisplatin of 0.25 µg/ml+ capecitabine at 30 µg/ml) corresponding to the PIAF clinical protocol, apart from pegylated interferon [4]. Apoptosis was evaluated with FITC annexin V and propidium iodide (PI) kit for flow cytometry (Invitrogen, Molecular probes). After the incubation period, cells were harvested by trypsinisation; the cell suspensions were washed with cold PBS and centrifuged at 1000 rpm for 5 min. Cells were counted and resuspended in 100 µl binding buffer; 5µl FITC Annexin V and 1µl of PI were added to each sample. Samples were then incubated at room temperature in the dark for 15 min. After the incubation period, 400 µl of binding buffer were added, and samples were kept on ice until they were analyzed by a flow cytometer (BD FACSCanto™ II system) measuring the fluorescence emission at 530 nm and 575 nm using 488 nm excitation. For this technique, the cells that are negative to both PI and annexin V staining are the alive ones, the cells PI - negative and annexin V-positive staining are considered to be early apoptotic ones, and the cells PI - positive and annexin V-positive staining are those in the latest stages of apoptosis or dead.

Data analysis

Statistical significance values were obtained by a one-way analysis of variance (ANOVA) with a 95% confidence level using GraphPad Prism 5 statistics program (La Jolla, CA, USA). Data were analyzed using one-way ANOVA with the Dunnett`s multiple comparison test. Statistical significance was set at $p < 0.05$, and all experiments were performed in triplicate.

Results

Synthesis and characterization of the GNP based delivery system

GNPs-L-Aspartate nanostructures were prepared by a one-step synthesis based on the reduction of $HAuCl_4$ in the presence of L-Aspartate (Asp). Discrete networks were observed to form due to the nanoparticles' fusion, as seen in Fig.1. In the synthesis, Asp was both the reducing and the capping agent. In order to obtain these types of nanostructures, we used low concentrations of gold, $C=0.5x10^{-3}M$ and $C=1.5x10^{-3}$ M, respectively.

Aspartate molecules serve competitively both reduction and capping functions and are responsible for generating isotropy (after nucleation, growth is produced over all faces, spherical nanoparticles being formed) and a random attachment. This mechanism of growth and attachment leads to nanostructures as presented in Fig. 1. The formation of GNPs in solution was highlighted by color change, first pink (suggesting the beginning of the reduction process), then slowly changing to red due to the formation of peanut-shaped particles which further followed a linear aggregation into chains. Drug-delivery systems should be synthesized so much so that both the internalization and transport of the drug are highly efficient. The drug was loaded into the nanocarrier vectors (GNPs-Aspartate nanostructures) through noncovalent interactions between the aspartate molecules and functional groups of the drug. The formation of complexes between drug molecules and nanocarriers is more advantageous than the covalent conjugation approach due to the ease of fabrication and controllable loading efficiency.

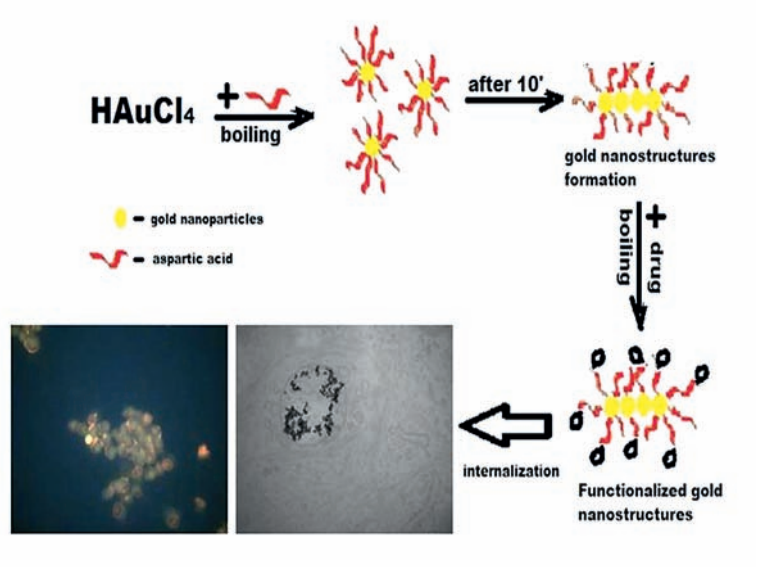

Fig 1. Mechanism of functionalization of gold nanostructure with the drugs (cisplatin/ capecitabine, and doxorubicin).

The morphology of the deliveries was revealed by using Transmission Electron Microscopy (TEM) (Fig. 2). It can be clearly seen that the GNPs-Aspartate structure has been rearranged by the presence of the drugs but maintains a nanometric size.

After binding the drug to the GNP, the broad band in the range of 3200–3700 cm^{-1} is due to the presence of surface-bound $–H_3$-N, –OH functionalities on the nanoparticle surface. This band overlaps with the –OH stretching vibration of the drug. The peaks that change position from 2980 to 2978 cm^{-1} represent the stretching vibration of C-H bonds from the rings. Also, the appearance of hydrogen bonds between the cytostatic and the carrier can be attributed to the bending vibration of N-H and stretching vibration of C=O, C-H, O-H. Their corresponding bands appear changed in frequency from 1722 to 1721 cm^{-1}. The band at about 1580 cm^{-1} is related to the ring breathing and appears in the spectrum unmodified. Carboxylate vibrations are visible for doxorubicin, for example, in the range of 1400–1445 cm^{-1} together with C–O–C asymmetric stretch at around 1284 cm^{-1}. Another change in position from 1076 cm^{-1} to 1073 cm^{-1} is attributed to the aliphatic CHX.

Cellular uptake of the drug

Since the cellular uptake efficiency of drug-loaded GNPs may affect the therapeutic benefits, confirmation of the presence of the cytostatic-loaded nanostructures is very important. Cells incubated with different drug combinations were studied, before optical microscopy images (white light microscopy and the corresponding images in fluorescence microscopy at 488 nm) were taken using a Zeiss Axiovert inverted phase microscope. Image acquisition was performed with an AxioCam MRC optical camera (Fig. 3 a-f).

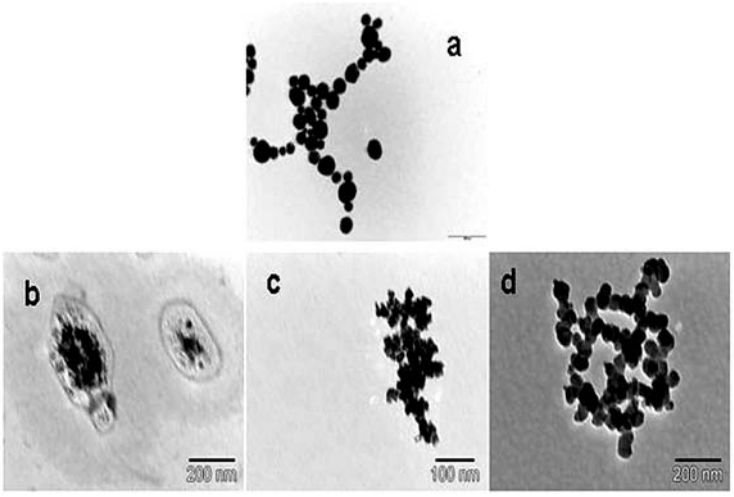

Fig 2. TEM images of gold nanostructure (a), gold nanostructure functionalized with cisplatin (b), capecitabine (c), doxorubicin (d).

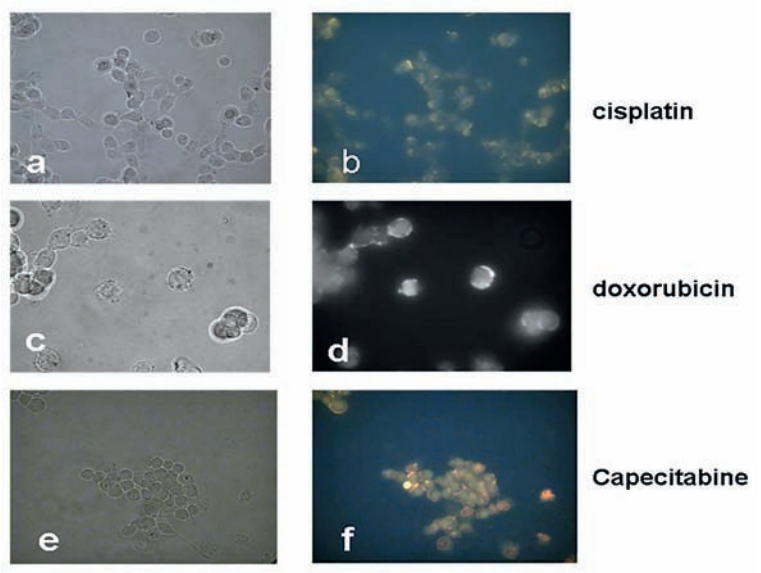

Fig 3. Drug-loaded nanoparticle intracellular accumulation on cancer cells (X100). Cisplatin: a) white light microscopy and b) fluorescence microscopy; doxorubicin: c) white light microscopy and d) fluorescence microscopy; capecitabine: e) white light microscopy and f) fluorescence microscopy.

In order to elucidate the mechanism of cell killing and to understand the efficiency of the delivery of the drugs to the CSC line, the cells were subsequently inspected by TEM. The TEM micrographs (after 1h of incubation) of the GNPs-drugs nanostructures in CSC cells are presented in Fig. 4. The route of uptake is a caveolin-dependent endocytosis followed by the release of the conjugated drugs from endosoms/lysosoms into the cells, where the reaction between cisplatin/doxorubicin/capecitabine and DNA occurs.

Figure 5 presents the visual differences between CSC, LIV, and HepG2 cells. It can be clearly seen that, in the case of HepG2 cells and CSC cells, the drug is more efficiently absorbed. If we analyze the different proliferation rates of the three cell types, we can observe the difference even macroscopically - a fact that may have great impact in the clinical management of liver cancer. Thus, after chemotherapy, according to our results, the normal liver parenchyma should be able to regenerate and substitute the tumor mass lyzed by the cytostatic regimen due to the surviving normal cancer cell population found in the canals of Hering [19]. The liver mass is not exclusively formed by hepatic progenitor cells, but also more differentiated hepatic cancer cells that may also divide and lead to clinical relapse. Nevertheless, the progenitor compartment is the most aggressive and definitely the most important target for future research in the field. The drugs' effects on different

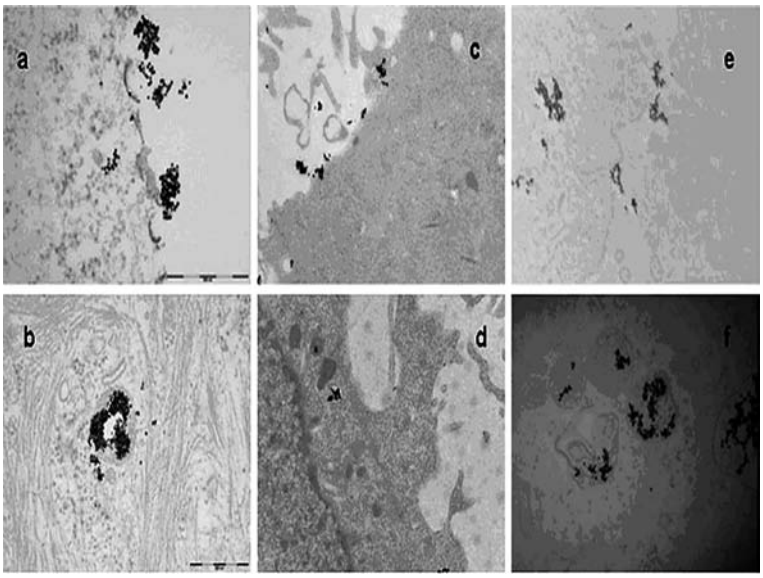

Fig 4. TEM micrographs of the drugs in CCS cells after 1 h of incubation: (a, b) GNPs-cisplatin, (c, d) GNPs -capecitabine (e, f) GNPs- doxorubicin.

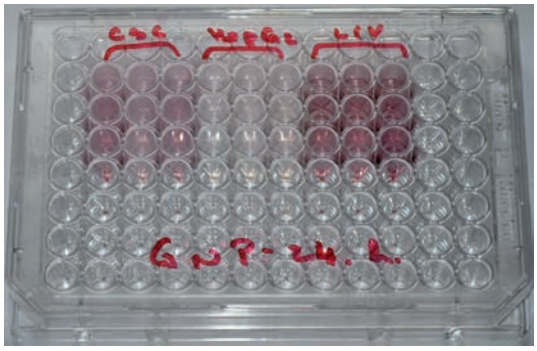

Fig 5. Visual observations of the differences in the MTT staining intensity values between CSC, LIV, and HepG2 cells; especially in the case of HepG2 cells and CSC cells, the drug was more efficient and induced visible changes in the intensity of the staining. The macrosopic visualization observations were confirmed by the MTT optical density values.

cells lines can be observed (after 24 hours) macroscopically on the culture flask, a difference also confirmed by the MTT assay.

Cytotoxicity assay

The cytotoxicity level induced by the various drug combinations was measured using the MTT assay, a very common method of evaluating the effects of different substances in cell cultures that is used to measure the cellular mitochondrial function of the cells in the culture dish. The concentrations of the different anticancer drugs used in this study were chosen in such a way that they would be readily and safely achievable in human patients, a statement that is supported by other studies previously cited in this manuscript and which first tested various drugs that belong to the PIAF protocol first *in vitro* and then *in vivo*, on either animal models or human subjects, with no or minimal side effects. Chemotherapy-resistant cells, in comparison with HepG2 cells, are resistant to the tested drugs - cisplatin, doxorubicin and capecitabine - but, when GNP-coated drugs are added to the culture media, the results show a significantly lower survival rate of the tumor cells at 48 hours. Using Dunnett's Multiple Comparison Test, statistically significant variations ($P<0.05$) as shown in Table I were found. Cell proliferation assays clearly demonstrate the differences between conventional chemotherapy and drug-loaded GNPs (Fig. 6).

Apoptosis flow cytometry analysis

Apoptosis-mediated cell death of LIV adult mesenchymal cells and CSC cells were examined by a double-staining method using FITC-labeled Annexin V/PI apoptosis detection kit and analyzed by flow cytometry. The cells were analyzed after 24 hours of exposure to a combination of drugs conjugated or unconjugated with GNP: doxorubicin + cisplatin + capecitabine, corresponding to the clinical chemotherapeutic PIAF protocol (Planning-, Information- and Analysis-System for Field Trials) (Cisplatin, Doxorubicin, 5-FU and Interferon) [4]. Apoptosis and cell death were high even in the control groups, possibly because of cell manipulation in the course of trypsinisation and transport on ice (Table II).

The percentage of total apoptotic cells (early apoptotic cells positive only for V annexin + late apoptotic and dead

Table I. Results of the statistical analysis of the experiment for the MTT assays in different conditions for the three cells lines investigated CSC, LIV, and HepG2

CSC No treatment vs. CSC GNP + Cisplatin	95% CI 0.07133 to 0.4533
CSC No treatment vs. CSC GNP + Doxorubicin	95% CI 0.08833 to 0.4703
CSC No treatment vs. CSC GNP + Capacitabine	95% CI 0.1380 to 0.5200
CSC No treatment vs GNP	95% CI -0.08267 to 0.2993
CSC. No treatment vs. CSC Cisplatin	95%CI -0.02167 to 0.3603
CSC No treatment vs. CSC Doxorubicin	95% CI -0.1020 to 0.2800
CSC No treatment vs. CSC Capacitabine	95% CI -0.07567 to 0.3063
HepG2 No treatment vs. HepG2 GNP + Cisplatin	95% CI 0.3246 to 0.5894
HepG2 No treatment vs. HepG2 GNP + Doxorubicin	95% CI 0.4462 to 0.7111
HepG2 No treatment vs. HepG2 GNP + Capacitabine	95% CI 0.3569 to 0.6218
HepG2 No treatment vs. HepG2 GNP	95% CI -0.02976 to 0.2351
HepG2. No treatment vs. HepG2 Cisplatin	95% CI 0.3769 to 0.6418
HepG2 No treatment vs.. HepG2 Doxorubicin	95% CI 0.1582 to 0.4231
HepG2 No treatment vs. . HepG2 Capacitabine	95% CI 0.1576 to 0.4224
LIV No treatment vs. LIV GNP + Cisplatin	95% CI 0.1221 to 0.3932
LIV No treatment vs. LIV GNP + Doxorubicin	95% CI 0.1055 to 0.3765
LIV No treatment vs LIV GNP + Capecitabine	95% CI 0.08213 to 0.3532
LIV No treatment vs LIV GNP	95% CI -0.09554 to 0.1755
LIV No treatment vs LIV +Cisplatin	95% CI 0.09180 to 0.3629
LIV No treatment vs LIV + Doxorubicin	95% CI 0.02913 to 0.3002
LIV No treatment vs LIV+ Capecitabin	95% CI 0.08546 to 0.3565

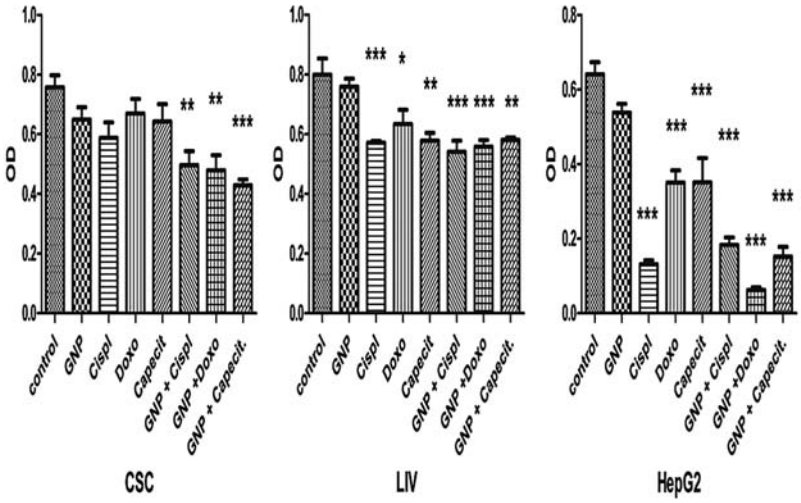

Fig 6. Experimental results of the MTT proliferation assay indicating the higher activity of the anticancer drugs in the presence of gold nanomaterials and various cancer lines.

Table II. Normal non-cancerous liver cells (LIV) and chemotherapy-resistent cancer cells (CSC) cells assessed for apoptosis by flow-cytometry measurements show an increased percentage of dead and apoptotic cells for the samples treated with GNP-conjugated drugs (GNP-PIAF) by comparison with the control group and cells treated with drugs alone

Sample	Early Apoptotic cells (%)	Late apoptotic +death cells (%)	Total apoptotic cells
LIV control	1.63	21.31	22.94
LIV treated with GNP-PIAF	1	60.3	61.3
LIV treated with PIAF	3.7	41.2	44.9
CSC control	9.7	6.2	15.9
CSC treated with GNP-PIAF	8	27.9	35.9
CSC treated with PIAF	0	26.1	26.1

cells positive for both V Annexin and PI) shows a greater apoptotic index for LIV cells, even in control samples, a slow increase in the proportion of apoptotic cells treated with drugs alone (1.1 folds in comparison with control group) and a greater increase in apoptotic cells treated with GNP-conjugated drugs (1.95 folds). CSC cells were therefore more sensitive to the chemotherapy treatment: the percentage of apoptotic and dead cells increased 1.64 folds in comparison with the control sample and 2.25 folds for GNP-conjugated drugs (Table II, Fig. 7). The greater apoptotic index of the control samples is actually a false-positive greater apoptotic index. Some of the cells died during sample manipulation stress such as trypsinization, centrifugation and the hypoxia conditions that cells were subjected to by transportation from the Department of Immunology at the Ion Chiricuta Cancer Center to the Laboratory of Cell Cytometry at the University of Veterinary Medicine and Agricultural Sciences, where the cell cycle analysis was carried out. Nevertheless, to assure that no differences existed between the cell subpopulations, all tubes were placed on ice and handled at the same time, under the exact same conditions.

Discussion

Medical research using GNP nanostructures is focused on biological and biomedical applications, such as imaging and drug/gene delivery, to treat various diseases. Most GNP conjugates are taken up by a non-specific mechanism, such as endocytosis and interaction with serum proteins, and it seems that the mechanism is dependent upon their size, shape, and surface chemistry [24].

Nanomaterials are known for their potential applications in various biomedical fields, including diagnostics and therapeutics [25,26]. We have shown in our study that GNPs can be explored to illustrate the mechanisms of biochemical modulation and have potentially a promising use in clinical liver cancer treatment.

Figure 4 shows the GNP conjugate to cisplatin, doxorubicin, and capecitabine uptake in live CSC cells after 24 hours of exposure to drugs. Phase contrast images and the corresponding images in 488nm fluorescence evidence perinuclear localization for GNPs-loaded with cisplatin and intracytoplasmic localization for GNP-doxorubicin and GNP-capecitabine conjugates in white light microscopy. Fluorescence images do not overlap the white light localization of GNPs, and the fluorescence intensity increased in the perimembrane space. An explanation can be found in the literature in which only GNP clusters of less than 4nm exhibited intrinsic fluorescence as previously reported [27,28].

Statistically significant data presented in the results show that in *in vitro* conditions, cytostatic drugs attached to GNPs are more efficient than the classic anticancer drugs. This may be partially due to the increased uptake of the drugs by the initial chemotherapy-resistant tumor cells. In addition, the activity of the multidrug resistance pump is slightly different in the case of chemotherapy-resistant cells in comparison

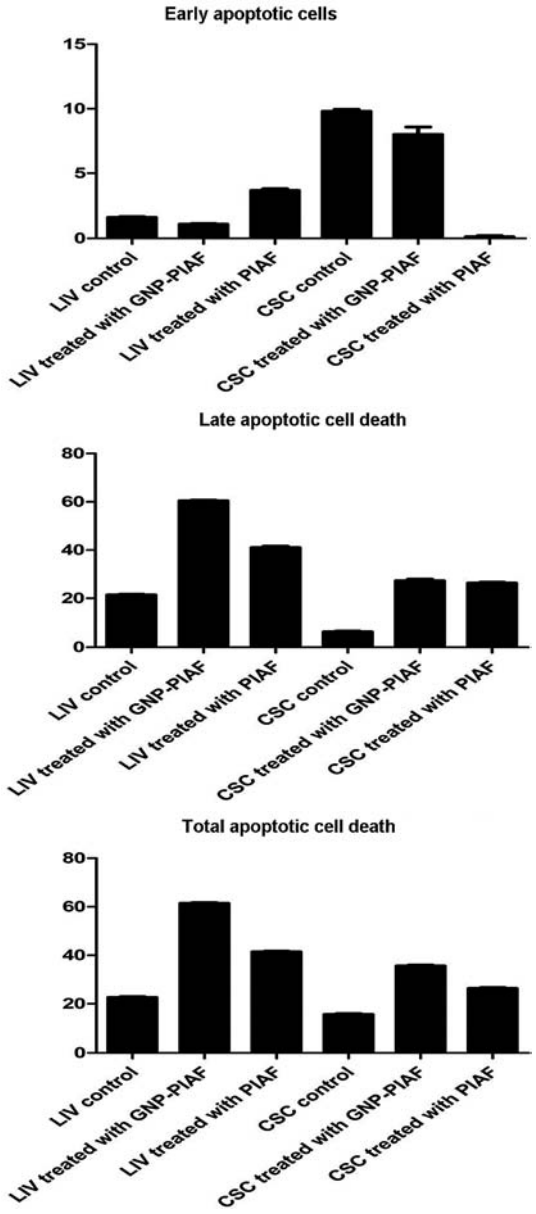

Fig 7. Graphic charts for the information in Table II, expressing early apoptotic cells (7A), late apoptotic cell death (7B) and total apoptotic cells (7C).

with more differentiated tumor cells, with tremendous potential for applications in oncology chemotherapy. Systemic chemotherapy for unresectable HCC has had a disappointing record of accomplishment, being unable to demonstrate a significant survival improvement [29]. Monotherapy with doxorubicin produces a response rate of 10-15% success, and a combination chemotherapy provides slightly better results, but without any significant survival benefits. The majority of HCC patients also have cirrhosis, which renders them unsuitable candidates for chemotherapy as the side effects associated with the cytotoxicity of anti-cancer drugs are likely to be worse [30].

In our study, in vitro cytotoxicity assay and V-Annexin/PI flow cytometry measurements of the apoptotic response of normal and tumor cells to the combination of chemotherapeutic drugs, alone or GNP-conjugated, revealed an increased toxicity for the regimen combining cisplatin, interferon, doxorubicin, and 5-fluorouracil (PIAF-protocol) GNP-conjugated. In clinical studies, positive responses have been reported in patients with HCC for this chemotherapeutic combination [31], but it produced more neutropenia, thrombocytopenia, and hypokalemia. This protocol may be considered for a selected subgroup of HCC patients, particularly those with preserved liver function in whom down-staging may be desired to facilitate future tumor resection [31-33]. Our results also show a different behavior between the normal and tumor cells, more evident in the case of a GNP-loaded drug. Underlying cirrhosis increases the risk of severe adverse effects as many cytostatic drugs are metabolized and eliminated via the liver. To improve both efficacy and safety, drug-delivery systems should include particulate carriers, such as liposomes, polymers, and nanoparticles, with the ultimate result being a significant increase in tumor drug concentration of up to 10-fold or even higher being achieved [34-36]. This approach will ensure administration of the same dose of conventional drugs to the cancer cells and tumors while leading to a decrease in the systemic side effects of present-day chemotherapy.

It is well-known that multidrug resistance, characterized by the over-expression of P-gp 170 that acts as an energy-dependent drug efflux pump and decreases cytotoxic drug accumulation, has been a major cause of failure in oncology leading to refractory disease and disseminated metastasis. As the primary approach to treating HCC is chemotherapy, a new strategy to target cancer cells is the administration of cytostatics using drug-carrier systems, such as liposomes or nanoparticles. Nanomaterials and GNPs, in particular, hold great promise in biomedical applications due to their high stability, low toxicity, and excellent biocompatibility. Therefore, given the additional ability to functionalize their surface with various drug molecules and biological vectors, as well as their ability to act as strong nanothermolysis agents for heat generation under electromagnetic excitations [37], GNPs constitute one of the most important engineered nanomaterials for bio-medical applications. The use of multifunctional nanoparticles as a platform technology to alter the chemoresistence of cancer cells to various cytostatic drugs could represent a simple yet efficient technique for treating inoperable cancers.

Conclusion

The current study demonstrates that functionalized nanoparticles can enable various drugs, cytostatics or antiviral drugs, to enter hepatic cancer cells at a higher concentration in comparison with differentiated tumor liver cells (HepG2 cells) and even in comparison with normal liver cells, allowing future therapeutics to effectively target the liver tumor and, at the same time, allow normal tissue to regenerate. The process must be further investigated to fully understand the exact mechanisms by which the presence of the GNPs seems to increase the activity of the

various drugs and to reduce the chemoresistance of the cells. These conjugated nanocomposites have significant potential applications in the treatment of hepatocellular carcinoma.

Conflicts of interest

No conflicts to declare.

Acknowledgements

The authors acknowledge funding from two grants of the Iuliu Hatieganu University and of the Ion Chiricuta Comprehensive Cancer Center, numbers 22714/37/06.10.2011 and 22714/38/06.10.2011, respectively. There are no conflicts of interest.

The authors gratefully acknowledge the invaluable help of Liliana Olenic (Department of Inorganic Chemistry, Faculty of Chemistry – Babes Bolyai University), Constantin Craciun (Center for Electron Microscopy at the Babes-Bolyai University in Cluj Napoca, Romania) and Alexandru Biris (Department of Nanotechnology – University of Arkansas, USA).

Both senior authors (IBD and AI) equally contributed to the current study.

References

1. Parkin DM, Bray F, Ferlay J, Pisani P. Estimating the world cancer burden: Globocan 2000. Int J Cancer 2001; 94: 153-156.
2. Bruix J, Sherman M; Practice Guidelines Committee, American Association for the Study of Liver Diseases. Management of hepatocellular carcinoma. Hepatology 2005; 42: 1208-1236.
3. Yang XR, Xu Y, Yu B, et al. High expression levels of putative hepatic stem/progenitor cell biomarkers related to tumour angiogenesis and poor prognosis of hepatocellular carcinoma. Gut 2010; 59: 953-962.
4. Yeo W, Mok TS, Zee B, et al. A randomized phase III study of doxorubicin versus cisplatin/Interferon α-2b/ Doxorubicin/ Fluorouracil (PIAF) combination chemotherapy for unresectable hepatocellular carcinoma. J Natl Cancer Inst 2005; 97: 1532-1538.
5. Miklášová N, Fischer-Fodor E, Lönnecke P, et al. Antiproliferative effect of novel platinum(II) and palladium(II) complexes on hepatic tumor stem cells in vitro. Eur J Med Chem 2012;49:41-47.
6. Forner A, Llovet JM, Bruix J. Hepatocellular carcinoma. Lancet 2012;379:1245-1255.
7. Singal AK, Anand BS. Management of hepatitis C virus infection in HIV/HCV co-infected patients: clinical review. World J Gastroenterol 2009; 15: 3713-3724.
8. Sharma P, Saini SD, Kuhn LB, et al. Knowledge of hepatocellular carcinoma screening guidelines and clinical practices among gastroenterologist. Dig Dis Sci 2011; 56: 569-577.
9. Jelic S, Sotiropoulos GC; ESMO Guidelines Working Group. Hepatocellular carcinoma: ESMO Clinical Practice Guidelines for diagnosis, treatment and follow-up. Ann Oncol 2010; 21 Suppl 5: v59-v64.
10. Riehle KJ, Dan YY, Campbell JS, Fausto N. New concepts in liver regeneration. J Gastroenterol Hepatol 2011; 26 Suppl 1: 203-212.
11. Mukherjee P, Bhattacharya R, Wang, et al. Antiangiogenic properties of gold nanoparticles. Clin Cancer Res 2005; 11: 3530-3534.
12. Sinha R, Kim GJ, Nie S, Shin DM. Nanotechnology in cancer therapeutics: bioconjugated nanoparticles for drug delivery. Mol Cancer Ther 2006; 5: 1909-1917.
13. Ghosh P, Han G, De M, Kim CK, Rotello VM. Gold nanoparticles in delivery applications. Adv Drug Deliv Rev 2008; 60: 1307-1315.
14. Bartczak D, Kanaras AG. Preparation of peptide functionalized gold nanoparticles using one pot EDC/sulfo-NHS coupling. Langmuir 2011; 27: 10119–10123.
15. Oh JH, Lee JS. Salt concentration-induced dehybridisation of DNA-gold nanoparticle conjugate assemblies for diagnostic applications. Chem Commun (Camb) 2010; 46: 6382-6384.
16. Yan B. Impacts of nanotechnology on medicinal chemistry and drug discovery. Curr Med Chem 2011; 18: 2044.
17. Lim ZZ, Li JE, Ng CT, Yung LY, Bay BH. Gold nanoparticles in cancer therapy. Acta Pharmacol Sin 2011; 32: 983-990.
18. Kudo M. The 2008 Okuda lecture: Management of hepatocellular carcinoma: from surveillance to molecular targeted therapy. J Gastroenterol Hepatol 2010; 25: 439-452.
19. Zhou H, Rogler LE, Teperman L, Morgan G, Rogler CE. Identification of hepatocytic and bile ductular cell lineages and candidate stem cells in bipolar ductular reactions in cirrhotic human liver. Hepatology 2007;45:716-724.
20. Tomuleasa C, Soritau O, Rus-Ciuca D, et al. Isolation and characterization of hepatic cancer cells with stem-like properties from hepatocellular carcinoma. J Gastrointestin Liver Dis 2010;19:61-67.
21. Wang P, Cong M, Liu TH, et al. Primary isolated hepatic oval cells maintain progenitor cell phenotypes after two-year prolonged cultivation. J Hepatol 2010;53:863-871.
22. Sasaki K, Kon J, Mizuguchi T, et al. Proliferation of hepatocyte progenitor cells isolated from adult human livers in serum-free medium. Cell Transplant 2008;17:1221-1230.
23. Wege H, Brümmendorf TH. Telomerase activation in liver regeneration and hepatocarcinogenesis: Dr. Jekyll or Mr. Hyde? Curr Stem Cell Res Ther 2007;2:31-38.
24. Lévy R, Shaheen U, Cesbron Y, Sée V. Gold nanoparticles delivery in mammalian live cells: a critical review. Nano Rev 2010; 1: 10.3402/nano.v1i0.4889.
25. Kah JC, Kho KW, Lee CG, et al. Early diagnosis of oral cancer based on the surface plasmon resonance of gold nanoparticles. Int J Nanomedicine 2007; 2: 785-798.
26. Ren L, Huang XL, Zhang B, et al. Cisplatin-loaded Au-Au2S nanoparticles for potential cancer therapy: cytotoxicity, in vitro carcinogenicity, and cellular uptake. J Biomed Mater Res A 2008; 85: 787-796.
27. Schaeffer N, Tan B, Dickinson C, et al. Fluorescent or not? Size-dependent fluorescence switching for polymer-stabilized gold clusters in the 1.1–1.7 nm size range. Chem Commun (Camb) 2008; 34: 3986–3988.
28. Guevel XL, Hotzer B, Jung G, Hollemeyer K, Trouillet V, Schneider M. Formation of fluorescent metal (Au, Ag) nanoclusters capped in bovine serum albumin followed by fluorescence and spectroscopy. J Phys Chem C 2011; 115: 10955–10963.
29. Wong R, Frenette C. Updates in the management of hepatocellular carcinoma. Gastroenterol Hepatol (N Y) 2011; 7: 16-24.
29. Rampone B, Schiavone B, Martino A, Viviano C, Confuorto G. Current management strategy of hepatocellular carcinoma. World J Gastroenterol 2009; 15: 3210-3216.
30. Leung TW, Patt YZ, Lau WY, et al. Complete pathological remission is possible with systemic combination chemotherapy for inoperable hepatocellular carcinoma. Clin Cancer Res 1999; 5: 1676–1681.
31. Yeo W, Mok TS, Zee B, et al. A randomized phase III study of doxorubicin versus cisplatin/interferon alpha-2b/doxorubicin/ fluorouracil (PIAF) combination chemotherapy for unresectable hepatocellular carcinoma. J Natl Cancer Inst 2005; 97: 1532–1538.
32. Quante M, Wang TC. Stem cells in gastroenterology and hepatology. Nat Rev Gastroenterol Hepatol 2009; 6: 724-737.

33. Nicolis SK. Cancer stem cells and “stemness” genes in neuro-oncology. Neurobiol Dis 2007; 25: 217-229.
34. Kettenbach J, Stadler A, Katzler IV, et al. Drug-loaded microspheres for the treatment of liver cancer: review of current results. Cardiovasc Intervent Radiol 2008; 31: 468-476.
35. Bae WK, Lee JH, Lee SJ, et al. Enhanced anti-cancer effect of 5-fluorouracil loaded into thermo-responsive conjugated linoleic acid-incorporated poloxamer hydrogel on metastatic colon cancer models. J Nanosci Nanotechnol 2011; 11: 1425-1428.
36. Xu Y, Mahmood M, Li Z, et al. Cobalt nanoparticles coated with graphitic shells as localized radio frequency absorbers for cancer therapy. Nanotechnology 2008; 19: 435102.
37. Mahmood M, Casciano DA, Mocan T, et al. Cytotoxicity and biological effects of functional nanomaterials delivered to various cell lines. J Appl Toxicol 2010; 30: 74-83.